Monatshefte für Chemie 137, 1385–1400 (2006)
DOI 10.1007/s00706-006-0539-4

Monatshefte für Chemie
Chemical Monthly
Printed in Austria

Novel Triplet Ground State Silylenes: H–N=C=Si, CN–N=C=Si, and *Me*O–N=C=Si at DFT Levels

Mohammed Z. Kassaee*, **Seyed M. Musavi, Foad Buazar,** and **Mehdi Ghambarian**

Department of Chemistry, University of Tarbiat Modarres, Tehran, Iran

Received March 13, 2006; accepted April 10, 2006
Published online October 27, 2006

Summary. DFT calculations predict the existence of three new triplet ground state silylenes: [(imino)-methylene]silylene, [(cyanoimino)methylene]silylene, and [(methoxyimino)methylene]silylene, with CNSi*X* formula (*X* = H, CN, and O*Me*, respectively). Discrepancies are found between DFT and some *ab initio* results.

Keywords. Triplet silylene; *Ab initio*; DFT; push-pull effect.

Introduction

The knowledge of the ground state spin, the singlet-triplet splitting ($\Delta E_{s\text{-}t}$), and the electronic effects of particular substituents on spin multiplicities and structures of divalent species is of great importance in understanding the chemistry of reactive intermediates [1–19]. The most well known highly reactive intermediates are carbenes (*X*–C–*Y*), which contain a divalent carbon with an unshared pair of electrons [1]. There are two low-lying states, singlet and triplet, depending on whether the electronic configuration is σ^2 or high spin $\sigma^1\pi^1$ [2, 3]. Whether the ground state of C*XY* is triplet or singlet is determined by the nature of substituents *X* and/or *Y* used. The singlet state is stabilized by both electron-withdrawing substituents and substituents donating p_π-lone pairs to the empty carbon p_π orbital. The triplet state is favored by substituents more electropositive than carbon and by sterically bulky substituents (which prefer large *X*–C–*Y* bond angles). Substituent effects on the addition of singlet carbenes to double bonds have been studied extensively [1–9]. In recent years, the chemistry of silylenes (the silicon analogues of carbenes) has also become of great theoretical and experimental interest [10–12]. Interesting bonding properties are shown for the silylenic isomers of C_2H_2Si and CNSiH,

* Corresponding author. E-mail: Kassaeem@Modares.ac.ir

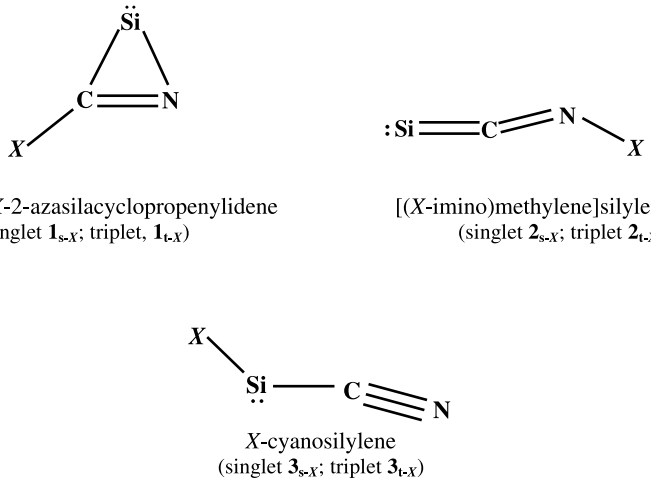

3-*X*-2-azasilacyclopropenylidene (singlet $\mathbf{1}_{s\text{-}X}$; triplet, $\mathbf{1}_{t\text{-}X}$)

[(*X*-imino)methylene]silylene (singlet $\mathbf{2}_{s\text{-}X}$; triplet $\mathbf{2}_{t\text{-}X}$)

X-cyanosilylene (singlet $\mathbf{3}_{s\text{-}X}$; triplet $\mathbf{3}_{t\text{-}X}$)

Fig. 1. The three possible structures of silylenic CNSi*X* isomers (**1**, **2**, and **3**) with the singlet (s) and/or triplet (t) states ($X = \mathrm{H}$, $\mathrm{NH_2}$, CN, O*Me*)

through their pioneering matrix isolation and characterization, by *G. Maier et al.* [13–15]. However, the question of electronic ground states of silylenes is still under very active investigation, because nearly all known silylenic species possess a singlet ground state [16, 17]. To address this question we have recently reported the singlet-triplet energy separations of halogenated C_2H_2Si silylenes [18]. Also, we have already studied the *ab initio* and DFT energetics of CNSi*X* halosilylenes where merely one triplet ground state silylene was found [19]. In attempt to increase the chances for triplet ground state silylenes the electronic effects of amino, cyano, and methoxy groups on the energy surface of CNSiH are examined (Fig. 1).

Results and Discussion

In order to have an overall insight, in this section first the results are listed, and then they are discussed. The singlet (s) and triplet (t) silylenes CNSi*X*, with the three possible structures 3-*X*-2-aza-1-silacyclopropenylidene (**1**), [(*X*-imino)methylene]-silylene (**2**), and X-cyanosilylene (**3**) are compared and contrasted, at seven levels of theory ($X = \mathrm{H}$, $\mathrm{NH_2}$, CN, and O*Me*) (Figs. 1–3, Tables 1–8). Relative energies of **1**–**3** are calculated using *B3LYP*, *MP*2, *MP*3, *MP*4 (SDTQ), and QCISD (T) methods with 6-31G*, 6-31G**, 6-311G**, and 6-311++G** basis sets (Tables 1–4). We have deliberately included data from several different levels of theory, since reporting the high as well as the low level calculations may offer an opportunity to compare various levels. It is noteworthy that for all the 24 CNSi*X* species the global minimum found by all calculation methods is $\mathbf{3}_{s\text{-}X}$ (Tables 1–4). *B3LYP*/6-311++G** calculated dipole moments and vibrational zero point energies (*ZPE*) are also presented in Tables 1–4. While energetic results appear dependent on the computational levels employed, neglecting $\mathbf{1}_{t\text{-}CN}$ as an exception, a relatively good consistency is found between the relative energies obtained through high level *MP*4 and QCISD(T), showing the highest difference of 12.55 kJ/mol. Besides having a good consistency with QCISD(T), the relatively higher level *MP*4

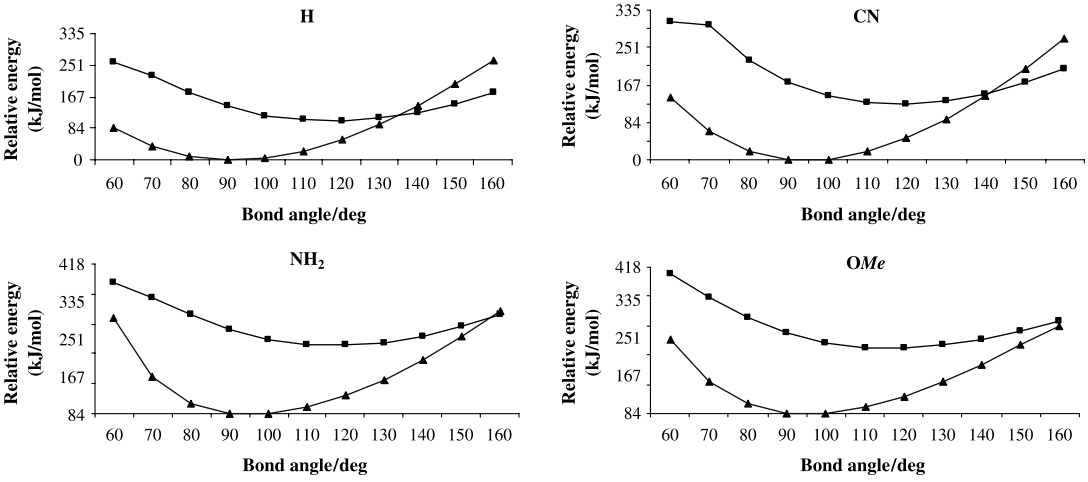

Fig. 2. Relative energies (kJ/mol) as a function of the divalent bond angle ∠*X*SiC (deg) (bending potential energy curves) for the singlet (▲) and triplet (■) states of *X*-cyanosilylene, $\mathbf{3}_{\mathbf{s}\text{-}X}$ and $\mathbf{3}_{\mathbf{t}\text{-}X}$, species ($X = $ H, CN, NH_2, and O*Me*)

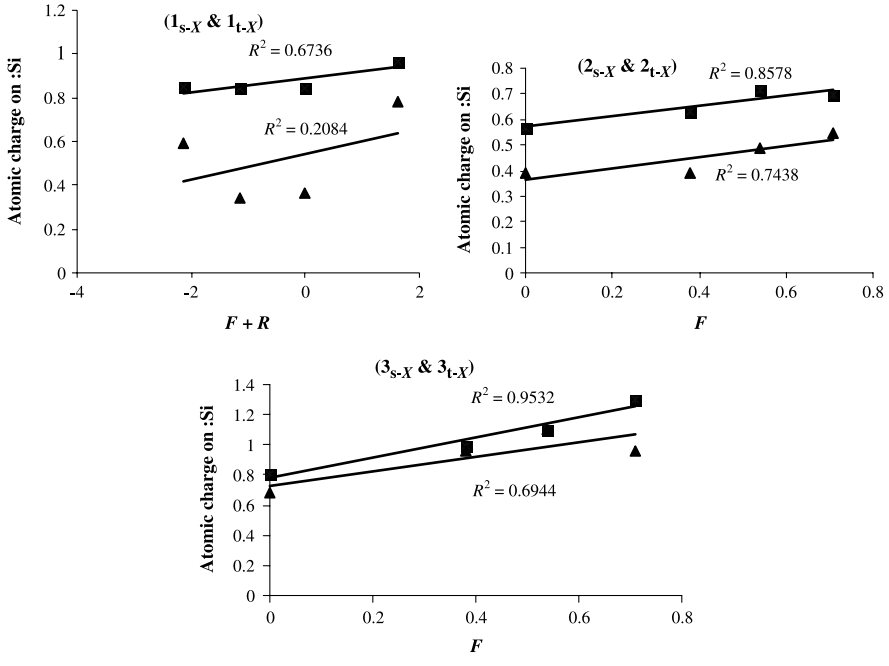

Fig. 3. Plots of atomic charge on silylenic center *vs. Swain* and *Lufton* constants [41] (*F*, *R*, and $F + R$) for singlet (■) and triplet (▲) CNSi*X* silylenes **1–3** where $X = $ H, CN, NH_2, and O*Me* (see Table 8)

(compared to *MP*2, *etc.*) appears to have acceptable $<S^2>$ expectation values [20, 21] for triplet states, showing the highest $<S^2>$ of 2.05 for the triplet $\mathbf{1}_{\mathbf{t}\text{-}\mathbf{CN}}$. Hence, the spin-contamination is not anticipated to be a problem for the species scrutinized.

Table 1. Relative energies (kJ/mol) for silylenic CNSiH singlet ($\mathbf{1_{s\text{-}H}}$, $\mathbf{2_{s\text{-}H}}$, and $\mathbf{3_{s\text{-}H}}$) and triplet states ($\mathbf{1_{t\text{-}H}}$, $\mathbf{2_{t\text{-}H}}$, and $\mathbf{3_{t\text{-}H}}$), including *ZPE* corrections, calculated at various levels of theory; along with *B3LYP*/6-311++G** computed dipole moments (D) and vibrational zero point energies (kJ/mol)

Structure	Relative energies (kJ/mol)						
	B3LYP/6-31G**	*MP*2/6-31G*	*MP*2/6-311G**[a]	*B3LYP*/6-311++G**	*MP*3/6-311G*[a]	*MP*4 (SDTQ)/6-311++G**[a]	QCISD (T)/6-311++G**[a]
$\mathbf{1_{s\text{-}H}}$	15.19	24.43	34.31	24.31	16.61	25.73	23.97
$\mathbf{1_{t\text{-}H}}$	164.47	195.35	208.11	174.31	218.95	201.17	195.06
$\mathbf{2_{s\text{-}H}}$	91.04	153.39	153.26	116.23	127.61	134.22	128.95
$\mathbf{2_{t\text{-}H}}$	89.24	140.54	145.90	93.97	122.09	154.60	138.41
$\mathbf{3_{s\text{-}H}}$[b]	0.00	0.00	0.00	0.00	0.00	0.00	0.00
$\mathbf{3_{t\text{-}H}}$	102.55	120.08	119.45	104.14	106.94	120.67	109.87

Structure	Dipole moments (D) *B3LYP*/6-311++G**	Vibrational zero point energies (kJ/mol) *B3LYP*/6-311++G**
$\mathbf{1_{s\text{-}H}}$	1.78	47.70
$\mathbf{1_{t\text{-}H}}$	2.31	42.22
$\mathbf{2_{s\text{-}H}}$	1.37	44.43
$\mathbf{2_{t\text{-}H}}$	2.22	43.64
$\mathbf{3_{s\text{-}H}}$	3.28	36.90
$\mathbf{3_{t\text{-}H}}$	3.67	37.49

[a] *ZPE* not included; [b] the lowest energy minimum set at 0.00 kJ/mol; total energies (hartrees) for $\mathbf{3_{s\text{-}H}}$ at various levels of theory sorted above: −382.8759504, −382.927531, −382.100284, −382.1660078, −382.1785822, −382.2121633, and −382.2101915

On the other hand, some *ab initio* results in Tables 1–4, are not in accord with the DFT conclusions. In particular, some of *MP*2, *MP*4, or QCISD(T) results suggest that the singlet state should be lower in energy than the corresponding triplet state even for [(imino)methylene]silylene, [(cyanoimino)methylene]silylene, and/or [(methoxyimino)methylene]silylene. We have drawn our conclusions mainly from the results of the DFT calculations based on the following three reasons. 1) To check the levels of confidence on our results, methods, and basis sets, the singlet-triplet splittings of divalent CH_2 and SiH_2 are calculated at various levels including our 7 employed levels in this paper (Appendix, Table A1). Results are compared and contrasted with those calculated at CASSCF for CH_2 and SiH_2 [23]. Interestingly, the closest results to the expensive CASSCF computations are those of *B3LYP*/6-311++G**. 2) Higher confidence is customarily placed on DFT calculations [24–32]. 3) Experimental results for silylenes and germylenes appear closest to DFT computations [13, 14, 33–40]. Hence, controversy introduced by some *ab initio* results in Tables 1–4 is resolved by adopting DFT as the method of choice in this paper.

Fully optimized geometrical parameters of **1**–**3** are reported, at *B3LYP*/6-311++G** and *MP*2/6-311G** levels of theory (Tables 5–7). Geometrical parameters obtained through other calculation methods have not much difference from those of *B3LYP*/6-311++G** and *MP*2/6-311G**, so for the sake of space they are not presented in Tables 5–7. With no exception, all optimized structures are

Table 2. Relative energies (kJ/mol) for silylenic $CNSiNH_2$ singlet ($\mathbf{1}_{s\text{-}NH_2}$, $\mathbf{2}_{s\text{-}NH_2}$, and $\mathbf{3}_{s\text{-}NH_2}$) and triplet states ($\mathbf{1}_{t\text{-}NH_2}$, $\mathbf{2}_{t\text{-}NH_2}$, and $\mathbf{3}_{t\text{-}NH_2}$), including *ZPE* corrections, calculated at various levels of theory; along with *B3LYP*/6-311++G** computed dipole moments (D) and vibrational zero point energies (kJ/mol)

Structure	Relative energies (kJ/mol)						
	B3LYP/ 6-31G**	*MP*2/ 6-31G*	*MP*2/ 6-311G**[a]	*B3LYP*/ 6-311++G**	*MP*3/ 6-311G*[a]	*MP*4 (SDTQ)/ 6-311++G**[a]	QCISD (T)/ 6-311++G**[a]
$\mathbf{1}_{s\text{-}NH_2}$	95.14	101.84	113.43	111.96	122.47	115.52	119.24
$\mathbf{1}_{t\text{-}NH_2}$	236.06	278.65	291.21	249.95	282.50	290.24	272.71
$\mathbf{2}_{s\text{-}NH_2}$	303.17	351.25	356.64	321.50	359.36	348.95	349.32
$\mathbf{2}_{t\text{-}NH_2}$	351.92	417.40	428.32	372.75	415.47	418.32	407.73
$\mathbf{3}_{s\text{-}NH_2}$[b]	0.00	0.00	0.00	0.00	0.00	0.00	0.00
$\mathbf{3}_{t\text{-}NH_2}$	221.67	222.51	221.71	224.60	227.94	234.72	230.33

Structure	Dipole moments (D) *B3LYP*/6-311++G**	Vibrational zero point energies (kJ/mol) *B3LYP*/6-311++G**
$\mathbf{1}_{s\text{-}NH_2}$	2.97	95.02
$\mathbf{1}_{t\text{-}NH_2}$	3.13	88.53
$\mathbf{2}_{s\text{-}NH_2}$	3.02	91.17
$\mathbf{2}_{t\text{-}NH_2}$	3.64	90.67
$\mathbf{3}_{s\text{-}NH_2}$	4.08	89.45
$\mathbf{3}_{t\text{-}NH_2}$	4.81	87.40

[a] *ZPE* not included; [b] the lowest energy minimum set at 0.00 kJ/mol; total energies (hartrees) for $\mathbf{3}_{s\text{-}NH_2}$ at various levels of theory sorted above: −438.2941751, −438.367451, −437.352881, −437.4518894, −437.4663737, −437.5149139, and −437.513321

planar with C_s symmetry. Atomic charges and bond orders are derived from the NBO population analysis at *B3LYP*/6-311++G** level (Table 8). The NBO method is preferred over *Mulliken* charges, since it provides an orbital picture which is closer to the classical *Lewis* structure. The magnitude of divalent bond angle is one of the most significant parameters which affect the magnitude of $\Delta E_{s\text{-}t}$ and the ground state of the divalent silylenes and/or carbenes [12]. That's why the divalent bond angle bending potential energy curves for acyclic structures $\mathbf{3}_{s\text{-}X}$ and $\mathbf{3}_{t\text{-}X}$ are calculated at *B3LYP*/6-311++G** (Fig. 2). The divalent angles ($\angle$XSiC) at which singlet $\mathbf{3}_{s\text{-}X}$ and triplet $\mathbf{3}_{t\text{-}X}$ states cross, appears as a function of *X*: O*Me* (>160°) > NH_2 (158°) > CN (136°) > H (130°). This trend follows the electronegativity of the atom directly attached to the divalent Si (Fig. 1). The NBO atomic charges on divalent Si atom of silylenic **1**–**3** are plotted against the *Swain* and *Lupton* constants [41] (Fig. 3). Force constant calculations show $\mathbf{1}_{t\text{-}NH_2}$, $\mathbf{2}_{s\text{-}NH_2}$, and $\mathbf{2}_{t\text{-}NH_2}$ to be transition states on the potential energy surface of $CNSiNH_2$ silylenes, since each possesses one imaginary frequency. Tables of DFT and *MP*2 calculated harmonic vibrational frequencies, pertaining to the four employed substituents (*X*), are omitted for the sake of brevity.

Considering the above results, the following three significant points are discussed: (a) the relative stabilities; (b) the singlet-triplet energy gaps, $\Delta E_{s\text{-}t}$, and (c) geometries, dipole moments, and atomic charges.

Table 3. Relative energies (kJ/mol) for silylenic CNSiCN singlet ($\mathbf{1}_{s\text{-}CN}$, $\mathbf{2}_{s\text{-}CN}$, and $\mathbf{3}_{s\text{-}CN}$) and triplet states ($\mathbf{1}_{t\text{-}CN}$, $\mathbf{2}_{t\text{-}CN}$, and $\mathbf{3}_{t\text{-}CN}$), including *ZPE* corrections, calculated at various levels of theory; along with *B3LYP*/6-311++G** computed dipole moments (D) and vibrational zero point energies (kJ/mol)

Structure	Relative energies (kJ/mol)						
	B3LYP/6-31G**	*MP2*/6-31G*	*MP2*/6-311G**[a]	*B3LYP*/6-311++G**	*MP3*/6-311G*[a]	*MP4* (SDTQ)/6-311++G**[a]	QCISD (T)/6-311++G**[a]
$\mathbf{1}_{s\text{-}CN}$	42.80	23.35	33.61	58.41	62.89	49.58	57.95
$\mathbf{1}_{t\text{-}CN}$	187.32	222.63	229.24	84.94	207.53	309.91	167.11
$\mathbf{2}_{s\text{-}CN}$	184.18	198.87	205.85	198.41	226.10	208.99	214.01
$\mathbf{2}_{t\text{-}CN}$	142.93	225.64	231.46	159.28	228.40	229.53	220.75
$\mathbf{3}_{s\text{-}CN}$[b]	0.00	0.00	0.00	0.00	0.00	0.00	0.00
$\mathbf{3}_{t\text{-}CN}$	195.14	193.38	193.34	196.48	197.82	204.97	198.91

Structure	Dipole moments (D) *B3LYP*/6-311++G**	Vibrational zero point energies (kJ/mol) *B3LYP*/6-311++G**
$\mathbf{1}_{s\text{-}CN}$	3.93	45.81
$\mathbf{1}_{t\text{-}CN}$	4.04	42.13
$\mathbf{2}_{s\text{-}CN}$	3.99	44.27
$\mathbf{2}_{t\text{-}CN}$	3.34	44.22
$\mathbf{3}_{s\text{-}CN}$	3.32	38.74
$\mathbf{3}_{t\text{-}CN}$	3.13	39.50

[a] *ZPE* not included; [b] the lowest energy minimum set at 0.00 kJ/mol; total energies (hartrees) for $\mathbf{3}_{s\text{-}CN}$ at various levels of theory sorted above: −475.1263195, −475.2060802, −474.1111645, −474.199615, −474.20947, −474.2725731, and −474.2684591

The Relative Stabilities

Due to the π-accepting character and strongly electron withdrawing effects of the CN group attached to the silylenic divalent center, singlet $\mathbf{3}_{s\text{-}X}$ appears to be the global minimum for all the 24 CNSi*X* species, at all theoretical levels employed (Tables 1–4). This is in contrast to the analogous C_2H_2Si isomers, where cyclic singlet state $\mathbf{1}_{s\text{-}H}$ was found to be more stable than the acyclic singlet state $\mathbf{3}_{s\text{-}H}$ by *Maier* [13–15] and us [18]. The relative stability for CNSiH isomers (*X*=H), calculated at *B3LYP*/6-311++G** level of theory is: $\mathbf{3}_{s\text{-}H}$ (0.00 kJ/mol) > $\mathbf{1}_{s\text{-}H}$ (24.31 kJ/mol) > $\mathbf{2}_{t\text{-}H}$ (93.97 kJ/mol) > $\mathbf{3}_{t\text{-}H}$ (704.14 kJ/mol) > $\mathbf{2}_{s\text{-}H}$ (116.23 kJ/mol) > $\mathbf{1}_{t\text{-}H}$ (174.31 kJ/mol) (Table 1). Excluding the global minimum $\mathbf{3}_{s\text{-}H}$ (discussed above), as a justification for the remaining of the above trend, one may point to the aromatic character of $\mathbf{1}_{s\text{-}H}$ caused by incorporating a σ^2 silylenic center within its continuously conjugated three membered ring. Similarly, $\mathbf{2}_{t\text{-}H}$ and $\mathbf{3}_{t\text{–}H}$ are less stable than $\mathbf{1}_{s\text{-}H}$ due to the lack of aromaticity. The intrinsic tendency of silylenes for having singlet ground states may be a good reason to justify the higher relative stability of $\mathbf{3}_{s\text{-}H}$ over $\mathbf{3}_{t\text{-}H}$ [23]. $\mathbf{2}_{t\text{-}H}$ is more stable than $\mathbf{3}_{t\text{-}H}$, probably due to the higher stability of the corresponding canonical forms for the former (Appendix, Figs. A1 and A2). One may justify the higher stability of $\mathbf{3}_{t\text{–}H}$ over $\mathbf{2}_{s\text{-}H}$ by considering the stabilizing effect of the C≡N group in $\mathbf{3}_{t\text{-}H}$.

Table 4. Relative energies (kJ/mol) for silylenic CNSiO*Me* singlet ($\mathbf{1}_{\mathbf{s\text{-}OMe}}$, $\mathbf{2}_{\mathbf{s\text{-}OMe}}$, and $\mathbf{3}_{\mathbf{s\text{-}OMe}}$) and triplet states ($\mathbf{1}_{\mathbf{t\text{-}OMe}}$, $\mathbf{2}_{\mathbf{t\text{-}OMe}}$, and $\mathbf{3}_{\mathbf{t\text{-}OMe}}$), including *ZPE* corrections, calculated at various levels of theory; along with *B3LYP*/6-311++G** computed dipole moments (D) and vibrational zero point energies (kJ/mol)

Structure	Relative energies (kJ/mol)						
	B3LYP/ 6-31G**	*MP*2/ 6-31G*	*MP*2/ 6-311G**[a]	*B3LYP*/ 6-311++G**	*MP*3/ 6-311G*[a]	*MP*4 (SDTQ)/ 6-311++G**[a]	QCISD (T)/ 6-311++G**[a]
$\mathbf{1}_{\mathbf{s\text{-}OMe}}$	139.37	163.01	162.84	148.36	150.67	155.73	153.89
$\mathbf{1}_{\mathbf{t\text{-}OMe}}$	127.82	373.05	–	331.58	357.06	366.81	357.69
$\mathbf{2}_{\mathbf{s\text{-}OMe}}$	374.13	437.69	435.64	383.42	414.13	411.33	404.30
$\mathbf{2}_{\mathbf{t\text{-}OMe}}$	205.64	230.75	–	201.29	213.43	494.84	–
$\mathbf{3}_{\mathbf{s\text{-}OMe}}$[b]	0.00	0.00	0.00	0.00	0.00	0.00	0.00
$\mathbf{3}_{\mathbf{t\text{-}OMe}}$	189.12	215.77	–	187.82	197.15	211.67	–

Structure	Dipole moments (D) *B3LYP*/6-311++G**	Vibrational zero point energies (kJ/mol) *B3LYP*/6-311++G**
$\mathbf{1}_{\mathbf{s\text{-}OMe}}$	3.59	136.02
$\mathbf{1}_{\mathbf{t\text{-}OMe}}$	3.94	132.72
$\mathbf{2}_{\mathbf{s\text{-}OMe}}$	0.86	131.50
$\mathbf{2}_{\mathbf{t\text{-}OMe}}$	2.19	130.67
$\mathbf{3}_{\mathbf{s\text{-}OMe}}$	5.02	131.42
$\mathbf{3}_{\mathbf{t\text{-}OMe}}$	4.64	130.58

[a] *ZPE* not included; [b] the lowest energy minimum set at 0.00 kJ/mol; total energies (hartrees) for $\mathbf{3}_{\mathbf{s\text{-}OMe}}$ at various levels of theory sorted above: −497.4693594, −497.5534511, −496.362922, −496.4896345, −496.5005753, −496.566410, and −496.56

The most interesting point to consider in the above relative energy trend is the higher stability of triplet state silylene $\mathbf{2}_{\mathbf{t\text{-}H}}$ over its corresponding singlet state $\mathbf{2}_{\mathbf{s\text{-}H}}$ by 22.24 kJ/mol. This higher stability of $\mathbf{2}_{\mathbf{t\text{-}H}}$ over $\mathbf{2}_{\mathbf{s\text{-}H}}$ is also confirmed by *B3LYP*/6-31G** (1.80 kJ/mol), *MP*2/6-31G* (12.85 kJ/mol), *MP*2/6-311G** (7.36 kJ/mol), and *MP*3/6-311G* (5.52 kJ/mol) levels (Table 1). This is in contrast to the reported intrinsic tendency of silylenes towards having more stable singlet states. Higher linearity of $\mathbf{2}_{\mathbf{t\text{-}H}}$ over $\mathbf{2}_{\mathbf{s\text{-}H}}$ as well as higher stability of the former through resonance may justify this incident. Finally, due to the enormous angle strains, cyclic $\mathbf{1}_{\mathbf{t\text{-}H}}$ turns out to be the least stable isomer in the CNSiH series.

Despite the force constant studies which show $\mathbf{2}_{\mathbf{s\text{-}NH_2}}$, $\mathbf{1}_{\mathbf{t\text{-}NH_2}}$ and $\mathbf{2}_{\mathbf{t\text{-}NH_2}}$ as transition states, the *B3LYP*/6-311++G** calculated order of relative stability for the possible structures on the energy surface of $CNSiNH_2$ is: $\mathbf{3}_{\mathbf{s\text{-}NH_2}}$ (0.00 kJ/mol) > $\mathbf{1}_{\mathbf{s\text{-}NH_2}}$ (111.96 kJ/mol) > $\mathbf{3}_{\mathbf{t\text{-}NH_2}}$ (224.60 kJ/mol) > $\mathbf{1}_{\mathbf{t\text{-}NH_2}}$ (249.95 kJ/mol) > $\mathbf{2}_{\mathbf{s\text{-}NH_2}}$ (321.50 kJ/mol) > $\mathbf{2}_{\mathbf{t\text{-}NH_2}}$ (372.75 kJ/mol) (Table 2). All singlet states appear more stable than their corresponding triplet states. In $CNSiNH_2$ structures the NH_2 group stabilizes the cyclic triplet $\mathbf{1}_{\mathbf{t\text{-}NH_2}}$ more than the transition state $\mathbf{2}_{\mathbf{t\text{-}NH_2}}$; this is in contrast to the CNSiH minima where $\mathbf{2}_{\mathbf{t\text{-}H}}$ is more stable than $\mathbf{1}_{\mathbf{t\text{-}H}}$. The range of energy differences in the case of $CNSiNH_2$ is wider compared to CNSiH. This is due to the strong electron releasing effects of the amino group which stabilizes the singlet state silylenes [12]. The electron

Table 5. Optimized geometrical parameters (bond lengths (R) and bond angles (A)) for singlet (s) and triplet (t) 3-*X*-2-aza-1-silacyclopropenylidene ($\mathbf{1}_{\mathbf{s}\text{-}X}$ and $\mathbf{1}_{\mathbf{t}\text{-}X}$) at two levels of theory: first line, *B3LYP*/6-311++G**; second line, *MP*2/6-311G** for $X = H$, NH_2, CN, and O*Me*

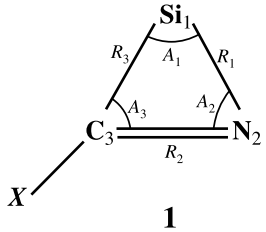

1

Structure ($\mathbf{1}_{\mathbf{s}\text{-}X}$ *vs.* $\mathbf{1}_{\mathbf{t}\text{-}X}$)	Bond lengths (Å)			Bond angles (deg)		
	R_1	R_2	R_3	A_1	A_2	A_3
$\mathbf{1}_{\mathbf{s}\text{-H}}$	1.82	1.29	1.81	41.4	68.8	69.8
	1.83	1.30	1.80	42.0	67.7	70.3
$\mathbf{1}_{\mathbf{s}\text{-NH}_2}$	1.78	1.31	1.82	42.7	70.5	66.7
	1.79	1.32	1.81	43.2	69.0	67.8
$\mathbf{1}_{\mathbf{s}\text{-CN}}$	1.82	1.29	1.82	41.7	69.1	69.2
	1.83	1.31	1.81	42.1	68.1	69.7
$\mathbf{1}_{\mathbf{s}\text{-O}Me}$	1.80	1.29	1.82	41.8	69.8	68.3
	1.81	1.30	1.80	42.2	68.5	69.2
$\mathbf{1}_{\mathbf{t}\text{-H}}$	2.19	1.21	2.05	32.8	67.4	79.7
	1.99	1.21	2.20	33.1	83.0	63.9
$\mathbf{1}_{\mathbf{t}\text{-NH}_2}$	–	–	–	–	–	–
	1.79	1.32	1.81	43.3	69.0	67.8
$\mathbf{1}_{\mathbf{t}\text{-CN}}$[a]	–	–	–	–	–	–
	1.69	1.37	2.03	42.0	82.5	55.5
$\mathbf{1}_{\mathbf{t}\text{-O}Me}$	1.98	1.22	2.10	34.6	78.4	67.0
	1.94	1.22	2.13	34.5	81.2	64.2

[a] Cyclic triplet geometries tend to rupture upon optimization

donating amino group on one side, along with the strongly electron withdrawing CN group on the other side of the divalent center makes $\mathbf{3}_{\mathbf{s}\text{-NH}_2}$ the global minimum for the set of $CNSiNH_2$ isomers (Fig. 1, Table 2). This result is indicated by all the employed calculation methods. In other words, in this situation one comes across with a ''push-pull'' case. Such a phenomenon apparently has more stabilizing effect on the open chain of the singlet $\mathbf{3}_{\mathbf{s}\text{-NH}_2}$, than aromaticity has on the strained three membered ring of $\mathbf{1}_{\mathbf{s}\text{-NH}_2}$. Nevertheless, when it comes to the case of triplet $\mathbf{3}_{\mathbf{t}\text{-NH}_2}$ (224.69 kJ/mol) *vs.* the singlet $\mathbf{1}_{\mathbf{s}\text{-NH}_2}$ (111.96 kJ/mol), aromaticity may justify the higher stability of the latter. Evidently, no possibility of the push-pull effect exists for the triplet $\mathbf{3}_{\mathbf{t}\text{-NH}_2}$.

The *B3LYP*/6-311++G** calculated relative order of stability for the six CNSiCN isomers is: $\mathbf{3}_{\mathbf{s}\text{-CN}}$ (0.00 kJ/mol) > $\mathbf{1}_{\mathbf{s}\text{-CN}}$ (58.41 kJ/mol) > $\mathbf{1}_{\mathbf{t}\text{-CN}}$ (84.94 kJ/mol) > $\mathbf{2}_{\mathbf{t}\text{-CN}}$ (159.28 kJ/mol) > $\mathbf{3}_{\mathbf{t}\text{-CN}}$ (196.48 kJ/mol) > $\mathbf{2}_{\mathbf{s}\text{-CN}}$ (198.41 kJ/mol) (Table 3). The range of energy differences in this trend is nearly the same as in the case of CNSiH, suggesting that the effects of the cyano group on the singlet

Table 6. Optimized geometrical parameters (bond lengths (R) and bond angles (A)) for singlet (s) and triplet (t) [(X-imino)methylene]silylene ($\mathbf{2_{s\text{-}X}}$ and $\mathbf{2_{t\text{-}X}}$) at two levels of theory: first line, *B3LYP*/6-311++G**; second line, *MP*2/6-311G** for X = H, NH_2, CN, and O*Me*

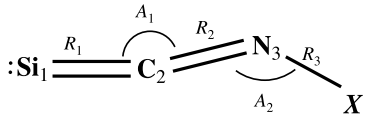

2

Structure ($\mathbf{2_{s\text{-}X}}$ *vs.* $\mathbf{2_{t\text{-}X}}$)	Bond lengths (Å)			Bond angles (deg)	
	R_1	R_2	R_3	A_1	A_2
$\mathbf{2_{s\text{-}H}}$	1.76	1.23	1.03	173.9	116.2
	1.75	1.25	1.03	174.1	113.5
$\mathbf{2_{s\text{-}NH_2}}$	1.70	1.30	1.32	174.8	121.2
	1.69	1.29	1.32	175.2	118.9
$\mathbf{2_{s\text{-}CN}}$	1.75	1.25	1.33	174.5	127.5
	1.75	1.26	1.35	174.6	121.5
$\mathbf{2_{s\text{-}OMe}}$	1.71	1.25	1.40	172.8	115.0
	1.71	1.27	1.38	173.1	114.1
$\mathbf{2_{t\text{-}H}}$	1.80	1.21	1.01	174.7	138.0
	1.82	1.12	1.00	175.5	141.5
$\mathbf{2_{t\text{-}NH_2}}$	1.78	1.21	1.39	174.1	140.5
	1.80	1.20	1.41	174.5	135.6
$\mathbf{2_{t\text{-}CN}}$	1.77	1.21	1.28	180.0	179.9
	1.80	1.21	1.34	175.6	140.4
$\mathbf{2_{t\text{-}OMe}}$	1.78	1.22	1.39	173.4	126.5
	1.81	1.20	1.38	173.4	131.5

and/or triplet states have equal weight. An interesting finding in the above trend is the higher stability of triplet state silylene $\mathbf{2_{t\text{-}CN}}$ over its corresponding singlet state $\mathbf{2_{s\text{-}CN}}$ by 39.13 kJ/mol. This higher stability is also confirmed by *B3LYP*/6-31G** (41.25 kJ/mol) while at *MP*3/6-311G* level this two isomer are isoenergetic (Table 3).

B3LYP/6-311++G** calculated order of relative stability for CNSiO*Me* isomers is: $\mathbf{3_{s\text{-}OMe}}$ (0.00 kJ/mol) > $\mathbf{1_{s\text{-}OMe}}$ (148.36 kJ/mol) > $\mathbf{3_{t\text{-}OMe}}$ (187.82 kJ/mol) > $\mathbf{2_{t\text{-}OMe}}$ (201.29 kJ/mol) > $\mathbf{1_{t\text{-}OMe}}$ (331.58 kJ/mol) > $\mathbf{2_{s\text{-}OMe}}$ (383.42 kJ/mol) (Table 4). This trend is different from that of CNSiH, CNSiCN, and/or $CNSiNH_2$ and a wider range of energy differences between the isomers is involved. Nevertheless, an interesting finding in this trend is the considerable higher stability of triplet state silylene $\mathbf{2_{t\text{-}OMe}}$ over its corresponding singlet state $\mathbf{2_{s\text{-}OMe}}$ (182.13 kJ/mol). This higher stability is also confirmed by *B3LYP*/6-31G** (168.49 kJ/mol), *MP*2/6-31G* (206.94 kJ/mol), and *MP*3/6-31G** (200.70 kJ/mol) (Table 4). This phenomenon may suggest that unlike the amino group, the methoxy has a higher resonance than inductive effect, since electronegativity increases the stability of singlet silylenes compared to the corresponding triplet states [23]. Again, the global minimum for the set of CNSiO*Me*

Table 7. Optimized geometrical parameters (bond lengths (R) and bond angles (A)) for singlet (s) and triplet (t) cyanosilylene ($\mathbf{3}_{\mathbf{s}\text{-}X}$ and $\mathbf{3}_{\mathbf{t}\text{-}X}$) at two levels of theory: first line, *B3LYP*/6-311++G**; second line, *MP*2/6-311G** for $X = $ H, NH_2, CN and O*Me*

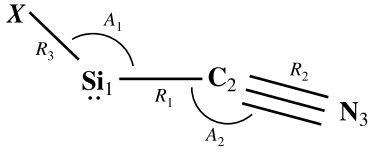

3

Structure ($\mathbf{3}_{\mathbf{s}\text{-}X}$ *vs.* $\mathbf{3}_{\mathbf{t}\text{-}X}$)	Bond lengths (Å)			Bond angles (deg)	
	R_1	R_2	R_3	A_1	A_2
$\mathbf{3}_{\mathbf{s}\text{-H}}$	1.88	1.16	1.52	91.5	173.2
	1.88	1.18	1.50	92.2	173.3
$\mathbf{3}_{\mathbf{s}\text{-NH}_2}$	1.91	1.16	1.72	95.1	172.0
	1.90	1.18	1.71	94.3	174.8
$\mathbf{3}_{\mathbf{s}\text{-CN}}$	1.88	1.16	1.88	94.2	170.0
	1.87	1.18	1.87	93.8	172.1
$\mathbf{3}_{\mathbf{s}\text{-O}\mathit{Me}}$	1.91	1.18	1.66	95.3	169.7
	1.90	1.18	1.65	95.0	172.4
$\mathbf{3}_{\mathbf{t}\text{-H}}$	1.81	1.16	1.48	116.9	176.2
	1.86	1.39	1.47	114.9	177.2
$\mathbf{3}_{\mathbf{t}\text{-NH}_2}$	1.82	1.16	1.73	116.2	175.5
	1.88	1.15	1.71	116.2	177.0
$\mathbf{3}_{\mathbf{t}\text{-CN}}$	1.80	1.16	1.80	117.5	174.9
	1.85	1.18	1.85	112.9	176.3
$\mathbf{3}_{\mathbf{t}\text{-O}\mathit{Me}}$	1.81	1.16	1.65	116.9	176.0
	1.87	1.14	1.64	115.4	175.7

silylenes, offered by all calculation methods appears to be singlet cyanosilylene $\mathbf{3}_{\mathbf{s}\text{-O}\mathit{Me}}$.

The Singlet-Triplet Energy Gaps

For cyclic structures consisting of singlet and/or triplet 3-*X*-2-azasilacyclopropenylidene, $\mathbf{1}_{\mathbf{s}\text{-}X}$ and/or $\mathbf{1}_{\mathbf{t}\text{-}X}$, respectively (where $X = $ H, CN, NH_2, and O*Me*), the *B3LYP*/6-311++G** calculated order of singlet-triplet energy gaps ($\Delta E_{\mathbf{s}\text{-}\mathbf{t},X}$) is: $\Delta E_{\mathbf{s}\text{-}\mathbf{t},\mathbf{O}\mathit{Me}}$ (183.22 kJ/mol) > $\Delta E_{\mathbf{s}\text{-}\mathbf{t},\mathbf{H}}$ (150.00 kJ/mol) > $\Delta E_{\mathbf{s}\text{-}\mathbf{t},\mathbf{NH_2}}$ (137.99 kJ/mol) > $\Delta E_{\mathbf{s}\text{-}\mathbf{t},\mathbf{CN}}$ (26.53 kJ/mol) (Tables 1–4). Excluding $\Delta E_{\mathbf{s}\text{-}\mathbf{t},\mathbf{NH_2}}$ which pertains to the energy difference between $\mathbf{1}_{\mathbf{s}\text{-}\mathbf{NH_2}}$ minimum and $\mathbf{1}_{\mathbf{t}\text{-}\mathbf{NH_2}}$ transition state, electron donating substituents appear to increase the stability of the corresponding singlet states and π-acceptor group CN stabilizes the triplet state more than the corresponding singlet states (Tables 1–4).

The first acyclic structure considered is [(*X*-imino)methylene]silylene (**2**) (Fig. 1). The order of energy gaps between $\mathbf{2}_{\mathbf{s}\text{-}X}$ and $\mathbf{2}_{\mathbf{t}\text{-}X}$ ($\Delta E_{\mathbf{s}\text{-}\mathbf{t},X}$), calculated at *B3LYP*/6-311++G** is: $\Delta E_{\mathbf{s}\text{-}\mathbf{t},\mathbf{O}\mathit{Me}}$ (−182.13 kJ/mol) > $\Delta E_{\mathbf{s}\text{-}\mathbf{t},\mathbf{NH_2}}$ (51.25 kJ/mol) > $\Delta E_{\mathbf{s}\text{-}\mathbf{t},\mathbf{CN}}$ (−39.13 kJ/mol) > $\Delta E_{\mathbf{s}\text{-}\mathbf{t},\mathbf{H}}$ (−22.26 kJ/mol) (Tables 1–4). Merely

Table 8. NBO analysis including atomic charges and bond orders of CNSi*X* ($X = H$, NH_2, CN, and O*Me*) silylenes in their three structures **1**–**3** calculated at *B3LYP*/6-311++G**

Structure	Species	Atomic charge				Bond order			
		Si	C	N	*X*	Si–N	Si–C	C–N	C–*X*
1	$\mathbf{1_{s\text{-}H}}$	0.846	−0.356	−0.681	0.191	–	–	–	–
	$\mathbf{1_{t\text{-}H}}$	0.361	−0.198	−0.392	0.229	–	–	–	–
	$\mathbf{1_{s\text{-}NH_2}}$	0.851	−0.028	−0.818	−0.780	0.88	0.72	1.77	1.22
	$\mathbf{1_{t\text{-}NH_2}}$	0.596	0.435	−0.965	−0.836	1.21	–	1.90	1.20
	$\mathbf{1_{s\text{-}CN}}$	0.966	−0.303	−0.638	0.225	0.80	0.73	1.89	1.12
	$\mathbf{1_{t\text{-}CN}}$	0.781	0.293	−0.926	0.089	1.37	–	1.65	1.53
	$\mathbf{1_{s\text{-}OMe}}$	0.843	0.087	−0.753	−0.527	–	–	–	–
	$\mathbf{1_{t\text{-}OMe}}$	0.342	0.383	−0.594	−0.508	–	–	–	–
						Si–C	C–N	N–*X*	
2	$\mathbf{2_{s\text{-}H}}$	0.568	−0.381	−0.538	0.352	1.47	1.89	0.82	
	$\mathbf{2_{t\text{-}H}}$	0.393	−0.205	−0.596	0.408	1.45	1.94	0.77	
	$\mathbf{2_{s\text{-}NH_2}}$	0.633	−0.644	−0.186	−0.549	1.43	1.83	1.42	
	$\mathbf{2_{t\text{-}NH_2}}$	0.392	−0.259	−0.264	−0.602	1.44	1.91	1.23	
	$\mathbf{2_{s\text{-}CN}}$	0.697	−0.361	−0.436	0.404	1.42	1.72	1.17	
	$\mathbf{2_{t\text{-}CN}}$	0.548	−0.223	−0.425	0.399	1.42	1.73	1.14	
	$\mathbf{2_{s\text{-}OMe}}$	0.718	−0.569	−0.094	−0.403	1.37	1.85	1.24	
	$\mathbf{2_{t\text{-}OMe}}$	0.485	−0.294	−0.154	−0.388	1.34	1.92	1.21	
						Si–*X*	Si–C	C–N	
3	$\mathbf{3_{s\text{-}H}}$	0.808	−0.269	−0.276	−0.262	0.70	0.65	2.50	
	$\mathbf{3_{t\text{-}H}}$	0.679	−0.265	−0.268	−0.146	0.91	0.92	2.50	
	$\mathbf{3_{s\text{-}NH_2}}$	0.995	−0.231	−0.317	−1.244	0.85	0.57	2.50	
	$\mathbf{3_{t\text{-}NH_2}}$	0.962	−0.245	−0.300	−1.210	0.95	0.90	2.50	
	$\mathbf{3_{s\text{-}CN}}$	1.302	0.372	−1.023	0.372	0.63	0.62	2.50	
	$\mathbf{3_{t\text{-}CN}}$	0.964	−0.252	−0.230	−0.252	0.87	0.86	2.51	
	$\mathbf{3_{s\text{-}OMe}}$	1.103	−0.247	−0.298	−0.893	0.10	1.37	1.85	
	$\mathbf{3_{t\text{-}OMe}}$	1.100	−0.280	−0.291	−0.874	0.84	0.93	2.50	

the high electron donating group NH_2 can reverse the negative sign of $\Delta E_{\mathbf{s\text{-}t},X}$ for structure **2**. Once more, this result demonstrates the stabilization of the singlet silylenes, due to both the electronegativity and resonance [42, 43]. Interestingly, all found triplet ground state silylenes belong to the acyclic structure **2**.

All singlet $\mathbf{3_{s\text{-}X}}$ are more stable than their corresponding triplet states $\mathbf{3_{t\text{-}X}}$ (Fig. 1). This is due to the singlet stabilizing C≡N motif which is directly attached to the divalent center of these acyclic structures. The *B3LYP*/6-311++G** calculated order of $\Delta E_{\mathbf{s\text{-}t},X}$ for $\mathbf{3_{s\text{-}X}}$ and $\mathbf{3_{t\text{-}X}}$ is: $\Delta E_{\mathbf{s\text{-}t,NH_2}}$ (224.60 kJ/mol) > $\Delta E_{\mathbf{s\text{-}t,CN}}$ (196.48 kJ/mol) > $\Delta E_{\mathbf{s\text{-}t,OMe}}$ (187.82 kJ/mol) > $\Delta E_{\mathbf{s\text{-}t,H}}$ (104.14 kJ/mol) (Tables 1–4). Evidently, electronic effects exerted by non-hydrogen substituents *X* (compared to hydrogen) on $\Delta E_{\mathbf{s\text{-}t},X}$ are more pronounced for structure **3** than either **2** or **1**. The amino group has the highest $\Delta E_{\mathbf{s\text{-}t}}$ among the cyanosilylene structures **3**. The methoxy group stabilizes the triplet state more than the corresponding singlet state in structure **2**. In contrast, in structure **3**, the methoxy group exceedingly stabilizes singlet state silylenes. The 4 singlet $\mathbf{3_{s\text{-}X}}$ acyclic cyano-

silyenes appear as the global minima among the 24 silylenic structures **1**–**3** which are scrutinized in this paper. This is in clear contrast to the analogous monohalogenated C_2H_2Si species which are reported to have the singlet cyclic aromatic structures $\mathbf{1}_{\mathbf{s\text{-}}X}$ as the global minima [18].

Geometries, Dipole Moments, and Atomic Charges

All the 24 optimized structures have a planar geometry with C_s symmetry. In contrast to the classic records of many silylenes, where the singlet divalent angle is often smaller than the corresponding triplet divalent angle [18, 21], the singlet states $\mathbf{1}_{\mathbf{s\text{-}H}}$ and $\mathbf{1}_{\mathbf{s\text{-}O}\boldsymbol{Me}}$ have larger divalent angles ($\angle A_1$) than their corresponding triplet states $\mathbf{1}_{\mathbf{t\text{-}H}}$ and $\mathbf{1}_{\mathbf{t\text{-}O}\boldsymbol{Me}}$, respectively (Table 5). Contrarily, highly strained triplet states $\mathbf{1}_{\mathbf{t\text{-}NH_2}}$ and $\mathbf{1}_{\mathbf{t\text{-}CN}}$, which are actually ruptured upon optimization, show larger divalent angles ($\angle A_1$) than their corresponding singlet states $\mathbf{1}_{\mathbf{s\text{-}NH_2}}$ and $\mathbf{1}_{\mathbf{s\text{-}CN}}$, respectively. Changes in geometrical parameters of the cyclic structures $\mathbf{1}_{\mathbf{s\text{-}}X}$ and $\mathbf{1}_{\mathbf{t\text{-}}X}$ as a function of X are negligible (Table 5). Nevertheless, in $\mathbf{2}_{\mathbf{s\text{-}}X}$ series the changes in geometrical parameters of the acyclic structures $\mathbf{2}_{\mathbf{s\text{-}}X}$ and $\mathbf{2}_{\mathbf{t\text{-}}X}$ as a function of X are somewhat significant. For instance the trend of R_1 bond length in $\mathbf{2}_{\mathbf{s\text{-}}X}$ series is: $\mathbf{2}_{\mathbf{s\text{-}H}} > \mathbf{2}_{\mathbf{s\text{-}CN}} > \mathbf{2}_{\mathbf{s\text{-}O}\boldsymbol{Me}} > \mathbf{2}_{\mathbf{s\text{-}NH_2}}$, while the trend of R_2 bond length is the opposite: $\mathbf{2}_{\mathbf{s\text{-}NH_2}} > \mathbf{2}_{\mathbf{s\text{-}O}\boldsymbol{Me}} > \mathbf{2}_{\mathbf{s\text{-}CN}} > \mathbf{2}_{\mathbf{s\text{-}H}}$ (Table 6). These trends may be justified by considering the possible canonical forms of the species involved (Appendix, Figs. A1 and A2). For example in $\mathbf{2}_{\mathbf{s\text{-}H}}$, R_1 is the longest while R_2 is the shortest, possibly due to the higher significance of a zwitterionic canonical form that enjoys a single bonded R_1 and triple bonded R_2. This is in contrast to $\mathbf{2}_{\mathbf{s\text{-}NH_2}}$, where a zwitterionic canonical form that possesses a triple bonded R_1 and a single bonded R_2 is of more significance. The cumulated bonds angle (N=C=Si, $\angle A_1$) in triplet $\mathbf{2}_{\mathbf{t\text{-}}X}$ tend to be linear (Table 6). In singlet $\mathbf{3}_{\mathbf{s\text{-}}X}$, the R_1 bond lengths are about 0.07–0.09 Å longer than those in the corresponding triplet structures $\mathbf{3}_{\mathbf{t\text{-}}X}$ (Table 7). The order of changes in R_1 bond lengths for $\mathbf{3}_{\mathbf{s\text{-}}X}$ structures is: $\mathbf{3}_{\mathbf{s\text{-}O}\boldsymbol{Me}} \approx \mathbf{3}_{\mathbf{s\text{-}NH_2}} > \mathbf{3}_{\mathbf{s\text{-}CN}} \approx \mathbf{3}_{\mathbf{s\text{-}H}}$. One may justify this observation by considering the involvement of a more significant zwitterionic canonical form which has a triple bonded R_2 and a single bonded R_1 in $\mathbf{3}_{\mathbf{s\text{-}NH_2}}$ as well as $\mathbf{3}_{\mathbf{s\text{-}O}\boldsymbol{Me}}$ (Appendix, Figs. A1 and A2). Such a zwitterionic canonical form is unacceptable for neither $\mathbf{3}_{\mathbf{s\text{-}CN}}$ nor $\mathbf{3}_{\mathbf{s\text{-}H}}$. However, R_2 bond lengths in $\mathbf{3}_{\mathbf{t\text{-}}X}$ have no noticeable sensitivity towards changes of substituents X. As expected, $\angle A_1$ divalent bond angles in all singlet $\mathbf{3}_{\mathbf{s\text{-}}X}$ species are smaller than those in their corresponding triplet states $\mathbf{3}_{\mathbf{t\text{-}}X}$. Depending on X, the order of changes in the bond angle $\angle A_1$ for $\mathbf{3}_{\mathbf{s\text{-}}X}$ is: $O\boldsymbol{Me} > NH_2 > CN > H$. In the case of $\mathbf{3}_{\mathbf{t\text{-}}X}$ this trend changes to: $CN > O\boldsymbol{Me} \approx H > NH_2$ (Table 7).

The order of dipole moments in CNSiH isomers is: $\mathbf{3}_{\mathbf{t\text{-}H}} > \mathbf{3}_{\mathbf{s\text{-}H}} > \mathbf{1}_{\mathbf{t\text{-}H}} > \mathbf{2}_{\mathbf{t\text{-}H}} > \mathbf{1}_{\mathbf{s\text{-}H}} > \mathbf{2}_{\mathbf{s\text{-}H}}$ (Table 1). Likewise, the order of dipole moments in $CNSiNH_2$ is: $\mathbf{3}_{\mathbf{t\text{-}NH_2}} > \mathbf{3}_{\mathbf{s\text{-}NH_2}} > \mathbf{1}_{\mathbf{s\text{-}NH_2}}$ (Table 2). The order of dipole moments in CNSiCN isomers is: $\mathbf{1}_{\mathbf{t\text{-}CN}} > \mathbf{2}_{\mathbf{s\text{-}CN}} > \mathbf{1}_{\mathbf{s\text{-}CN}} > \mathbf{2}_{\mathbf{t\text{-}CN}} > \mathbf{3}_{\mathbf{s\text{-}CN}} > \mathbf{3}_{\mathbf{t\text{-}CN}}$ (Table 3). Finally, the order of dipole moments in CNSiO*Me* isomers is: $\mathbf{3}_{\mathbf{s\text{-}O}\boldsymbol{Me}} > \mathbf{3}_{\mathbf{t\text{-}O}\boldsymbol{Me}} > \mathbf{1}_{\mathbf{t\text{-}O}\boldsymbol{Me}} > \mathbf{1}_{\mathbf{s\text{-}O}\boldsymbol{Me}} > \mathbf{2}_{\mathbf{t\text{-}O}\boldsymbol{Me}} > \mathbf{2}_{\mathbf{s\text{-}O}\boldsymbol{Me}}$ (Table 4). The highest dipole moments are encountered for $\mathbf{3}_{\mathbf{s\text{-}}X}$ and $\mathbf{3}_{\mathbf{t\text{-}}X}$ species when $X = NH_2$, O*Me*, and H. However, the symmetrical N≡C–Si–C≡N arrangement in $\mathbf{3}_{\mathbf{s\text{-}CN}}$ and $\mathbf{3}_{\mathbf{t\text{-}CN}}$ considerably lowers the dipole moments in these isomers to an extent that they appear as the lowest polar species

in the CNSiCN series (Fig. 1). Moreover, the structure with the largest dipole moment (5.02 D) appears to be $\mathbf{3}_{\mathbf{s}\text{-}OMe}$. This is possibly due to a push-pull direct resonance between O*Me* and CN groups, described in a polar zwitterionic canonical form (Appendix, Schemes A1 and A2).

The NBO analysis revealed that silylenic divalent centers in all species are positive (Table 8). One way to justify the variation of charge on Si, as a function of substituents, is to draw plots of atomic charges on Si atom against *Swain* and *Lupton* constants [26] (Fig. 3). These constants are polar (F), resonance (R), and sum of polar and resonance constants ($F+R$) and the silylenic structures considered are **1**–**3**. Among these plots that involving the atomic charges on the divalent Si atoms of $\mathbf{1}_{\mathbf{s}\text{-}X}$ *vs.* $F+R$ constants appear to have linear relationship, assuming comparable weighting factors ($f \approx r \approx 1$). However, $\mathbf{1}_{\mathbf{t}\text{-}X}$, $\mathbf{2}_{\mathbf{s}\text{-}X}$, $\mathbf{2}_{\mathbf{t}\text{-}X}$, $\mathbf{3}_{\mathbf{s}\text{-}\mathbf{X}}$, and $\mathbf{3}_{\mathbf{t}\text{-}X}$ fail to show such linear relationships between the atomic charges on Si and $F+R$, possibly due to the higher differences between their corresponding empirical sensitivities f and r. Instead, the atomic charges on Si of these acyclic species, show rather good linear relationships with polar constant (F). This indicates the higher importance of polar effects over the resonance effects in $\mathbf{2}_{\mathbf{s}\text{-}X}$, $\mathbf{2}_{\mathbf{t}\text{-}X}$, $\mathbf{3}_{\mathbf{s}\text{-}\mathbf{X}}$, and $\mathbf{3}_{\mathbf{t}\text{-}X}$ (Fig. 1).

Computational Methods

All calculations are performed using the Gaussian 98 program package [44]. The geometries and energetics are calculated using standard quantum chemical *ab initio* and DFT methods. All geometries are fully optimized without imposing any symmetry constraints; although, in some instances, the resulting structures show various elements of symmetry. For DFT calculations the *Becke*'s hybrid three-parameter functional combined with the *Lee-Yang-Parr* nonlocal correlation [45] with the 6-31G** and 6-311++G** basis sets are used [46]. For the second-order *Møller-Plesset* (*MP*2) method, the 6-31G* and 6-311G** basis sets are used. While, for the third-order *Møller-Plesset* (*MP*3) method, the 6-311G* basis set is employed [47, 48]. Singlet states are calculated with spin-restricted wave functions. The *MP*2/6-311G** optimized geometries are submitted as input for single-point calculations at the fourth-order *MP*4/6-311++G** and QCISD(T)/6-311++G** levels [49–51]. Single-point calculations are performed to improve *ab initio* energetic results. To predict the singlet-triplet energy differences more reliably the spin projected wave functions are employed for triplet states. The harmonic vibrational frequencies and zero point energies (*ZPE*) of these isomers are calculated at *B3LYP*/6-311++G** and *MP*2/6-311G** levels. The vibrational frequencies and *ZPE* data at the *B3LYP* and *MP*2 are scaled by 0.98 and 0.92, respectively [52, 53]. The NBO population analysis are accomplished at the *B3LYP*/6-311++G** level [54].

Acknowledgements

We are grateful to *A. Ghaderi* (Chemistry Department, Imam Hossein University) for many stimulating and helpful discussions. We also thank Dr. *Y. Fatholahi* (Tarbiat Modares University) for his cordial collaborations.

Appendix

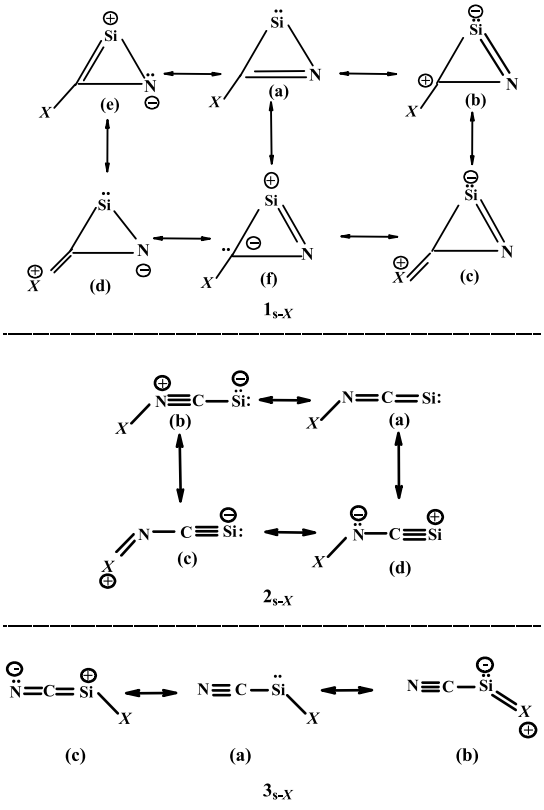

Fig. A1. Resonance canonical forms for singlet states silylenes $\mathbf{1}_{s\text{-}X}$, $\mathbf{2}_{s\text{-}X}$, and $\mathbf{3}_{s\text{-}X}$

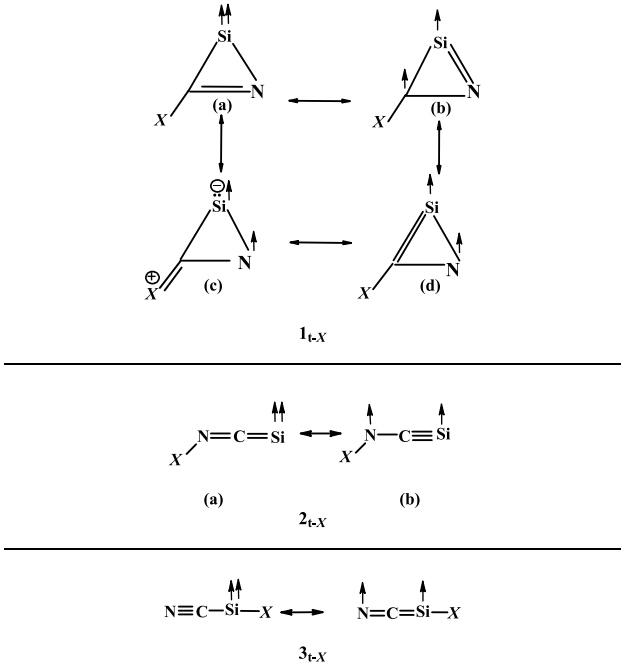

Fig. A2. Resonance canonical forms for triplet state silylenes $\mathbf{1}_{t\text{-}X}$, $\mathbf{2}_{t\text{-}X}$, and $\mathbf{3}_{t\text{-}X}$

Table A1. Relative singlet (s)-triplet (t) energy gaps (kJ/mol) for CH_2 and SiH_2, calculated at 16 levels of theory along with *ZPE* corrections

	B1LYP/6-31++G**	*B1LYP*/6-311++G**	*B3LYP*/6-31++G**	*B3LYP*/6-311++G**	*HF*/6-31++G**	*HF*/6-311++G**	*MP2*/6-31++G**	*MP2*/6-311++G**
CH_2-s	–	50.21	51.46	49.25	–	119.03	76.73	71.17
CH_2-t	–	0.00	0.00	0.00	–	0.00	0.00	0.00
SiH_2-s	0.00	–	0.00	0.00	0.00	0.00	0.00	0.00
SiH_2-t	84.27	–	84.98	85.40	19.96	19.62	58.12	60.04

	MP3/6-31++G**	*MP3*/6-311++G**	*MP4*(STDQ)/6-311++G**	QCISD(T)/6-311++G**	CCSD(T)/6-311++G**	G1	G2
CH_2-s	68.28	62.17	57.03	50.71	50.71	26.02	27.87
CH_2-t	0.00	0.00	0.00	0.00	0.00	0.00	0.00
SiH_2-s	0.00	0.00	0.00	0.00	0.00	0.00	0.00
SiH_2-t	67.40	69.41	73.47	76.11	76.11	99.16	97.70

References

[1] Kirmse W (1971) Carbene Chemistry; Academic Press, New York
[2] Moss RA, Jones M (eds) (1975) Carbenes Vol. 2. Wiley, New York
[3] Moss RA, Jones M (eds) (1985) Reactive Intermediates Wiley, New York
[4] Goddard WA, Dunning TH Jr, Hunt WJ, Hay PJ (1973) Acc Chem Res **6**: 368
[5] Bauschlicher CW Jr, Schaefer III HF, Bagus PS (1977) J Am Chem Soc **99**: 7106
[6] Harrison JF, Liedtke RC, Liebman JF (1979) J Am Chem Soc **101**: 7162
[7] Carter EA, Goddard WA (1988) J Chem Phys **88**: 1752
[8] Moss RA (1980) Acc Chem Res **13**: 58
[9] Moss RA (1989) Acc Chem Res **22**: 15
[10] Apeloig Y (1989) In: Patai S, Rappoport Z (eds) The Chemistry of Organic Silicon Compounds; John Wiley & Sons Ltd, New York, Chapter 2
[11] Gaspar PP, West R (1998) In: Rappoport Z, Apeloig Y (eds) The Chemistry of Organic Silicon Compounds II; John Wiley & Sons Ltd, New York, Chapter 43
[12] Gaspar PP, Xiao M, Pae DH, Berger DJ, Haile T, Chen T, Lei D, Winchester WR, Jiang P (2002) J Organomet Chem **646**: 68
[13] Maier G, Reisenauer HP, Egenolf H, Glatthaar J (1998) Eur J Org Chem: 1307
[14] Maier G, Reisenauer HP, Egenolf H, Meudt A (1998) Eur J Org Chem: 1313
[15] Maier G, Reisenauer HP, Schwab W, Carsky P, Hess BA, Schaad LJ (1987) J Am Soc **109**: 5183
[16] Pae DH, Xiao M, Chiang MY, Gaspar PP (1991) J Am Chem Soc **113**: 1281
[17] Gaspar PP, Beatty AM, Chen T, Haile T, Lei D, Winchester WR, Braddock-Wilking J, Rath NP, Klooster WT, Koetzle TF, Mason SA, Albinati A (1999) Organometallics **18**: 3921
[18] Kassaee MZ, Musavi SM, Buazar F, Ghambarian M (2005) J Mol Struct (Theochem) **722**: 151
[19] Kassaee MZ, Musavi SM, Hamadi H, Ghambarian M, Hosseini SE (2005) J Mol Struct (Theochem) **730**: 33
[20] Aoki K, Ikuta S, Murakami A (1996) J Mol Struct (Theochem) **365**: 103
[21] Barrientos C, Cimas A, Largo A (2001) J Phys Chem A **105**: 6724
[22] Nicolaides A, Nakayama T, Yamazaki K, Tomioka H, Koseki S, Stracener LL, McMahon RJ (1999) J Am Chem Soc **121**: 10563
[23] Apeloig Y, Pauncz R, Karni M, West R, Steiner W, Chapman D (2003) Organometallics **22**: 3250
[24] Ghanty TK, Ghosh SK (2002) J Phys Chem A **106**: 11815
[25] Parr RG, Yang W (1995) Annu Rev Phys Chem **46**: 701

[26] Pearson RG (1993) Acc Chem Res **26**: 250
[27] Ghanty TK, Ghosh SK (1994) J Am Chem Soc **116**: 3943
[28] Zhou Z, Parr RG (1990) J Am Chem Soc **112**: 5720
[29] Grafenstein J, Hjerpe AM, Kraka E, Cremer D (2000) J Phys Chem A **104**: 1748
[30] Enyo T, Nicolaides A, Tomioka T (2002) J Org Chem **67**: 5578
[31] Trindle C, Datta SN, Mallik B (1997) J Am Chem Soc **119**: 12947
[32] Worthington SE, Cramer CJ (1997) J Phys Org Chem **10**: 755
[33] Zemlyansky NN, Borisova IV, Khrustalev VN, Antipin MY, Ustynyuk YA, Nechaev MS, Lunin VV (2003) Organometallics **22**: 5441
[34] Yoshida M, Tamaoki N (2002) Organometallics **21**: 2587
[35] Tsutsui S, Tanaka H, Kwon E, Matsumoto S, Sakamoto K (2004) Organometallics **23**: 5659
[36] Joo H, McKee ML (2005) J Phys Chem A **109**: 3728
[37] Dhiman A, Muller T, West R, Becker JY (2004) Organometallics **23**: 5689
[38] Olah J, De Proft F, Veszpremi T, Geerlings P (2004) J Phys Chem A **108**: 490
[39] Koch R, Bruhn T, Weidenbruch M (2004) Organometallics **23**: 1570
[40] Kwon E, Tanaka H, Makino T, Tsutsui S, Matsumoto S, Segawa Y, Sakamoto K (2006) Organometallics **25**: 1325
[41] Swain CG, Lupton CE Jr (1968) J Am Chem Soc **90**: 4328
[42] Bourissou D, Guerret O, Gabbai FP, Bertrand G (2000) Chem Rev **100**: 39
[43] Arduengo III AJ (1999) Acc Chem Res **32**: 913
[44] Frisch MJ, Trucks GW, Schlegel HB, Scuseria GE, Robb MA, Cheeseman JR, Zakrzewski VG Jr, Montgomery JA, Stratmann RE, Burant JC, Dapprich S, Millan JM, Daniels AD, Kudin KN, Strain MC, Farkas O, Tomasi J, Barone V, Cossi M, Cammi R, Mennucci B, Pomelly C, Adamo C, Clifford S, Ochterski J, Petersson GA, Ayala PY, Cui Q, Morokuma K, Malick DK, Rabuck AD, Raghavachari K, Foresman JB, Cioslowski J, Ortiz JV, Baboul AG, Stefanov BB, Liu G, Liashenko A, Piskorz P, Komaromi I, Gomperts R, Martin RL, Fox DJ, Keith T, Al-Laham MA, Peng CY, Nanayakkara A, Gonzalez C, Challacombe M, Gill PMW, Johnson B, Chen W, Wong MW, Andres JL, Gonzalez C, Head-Gordon M, Replogle ES, Pople JA (1998) 98, Gaussian Inc, Revision A7, Pittsburgh, PA
[45] Becke AD (1996) J Chem Phys **104**: 1040
[46] Frisch MJ, Pople JA, Binkley JS (1984) J Chem Phys **80**: 3265
[47] Saebo S, Almlof J (1989) Chem Phys Lett **154**: 83
[48] Pople JA, Binkley JS, Seeger R (1976) Int J Quant Chem Symp **10**: 1
[49] Pople JA, Krishnan R (1978) Int J Quant Chem **14**: 91
[50] Krishnan R, Frisch MJ, Pople UJA (1980) J Chem Phys **72**: 4244
[51] Pople JA, Head-Gordon M, Raghavachari K (1987) J Chem Phys **87**: 5968
[52] Hout RF, Levi BA, Heher WJ (1985) J Comput Chem **82**: 234
[53] Defrees DJ, McLean AD (1985) J Chem Phys **82**: 333
[54] Carpenter JE, Weinhold F (1988) J Mol Struct (Theochem) **41**: 169